Thermal Conversion of Electronic and Electrical Properties of $AuCl_3$-Doped Single-Walled Carbon Nanotubes

Seon-Mi Yoon,[†,§] Un Jeong Kim,[†,§] Anass Benayad,[†] Il Ha Lee,[‡] Hyungbin Son,[†] Hyeon-Jin Shin,[†] Won Mook Choi,[†] Young Hee Lee,[‡] Yong Wan Jin,[†] Eun-Hong Lee,[†] Sang Yoon Lee,[†] Jae-Young Choi,*[,†] and Jong Min Kim*[,†]

[†]Samsung Advanced Institute of Technology, Yongin, Gyeonggi-do 446-71, Korea, and [‡]BK21 Physics Division, Sungkyunkwan Advanced Institute of Nanotechnology, Center for Nanotubes and Nanostructured Composites, Sungkyunkwan University, Suwon, Gyeonggi-do 440-746, Korea.
[§]These authors contributed equally to this work.

ABSTRACT By using carbon-free inorganic atomic layer involving heat treatment from 150 to 300 °C, environmentally stable and permanent modulation of the electronic and electrical properties of single-walled carbon nanotubes (SWCNTs) from p-type to ambi-polar and possibly to n-type has been demonstrated. At low heat treatment temperature, a strong p-doping effect from Au^{3+} ions to CNTs due to a large difference in reduction potential between them is dominant. However at higher temperature, the gold species are thermally reduced, and thermally induced CNT−Cl finally occurs by the decomposition reaction of $AuCl_3$. Thus, in the $AuCl_3$-doped SWCNTs treated at higher temperature, the p-type doping effect is suppressed and an n-type property from CNT−Cl is thermally induced. Thermal conversion of the majority carrier type of $AuCl_3$-doped SWNTs is systematically investigated by combining various optical and electrical tools.

KEYWORDS: carbon nanotubes · gold chloride · thermal treatment · doping · transistor

Single-walled carbon nanotubes (SWCNTs) have attracted tremendous attention due to their extraordinary electrical, physical, chemical, and thermal properties. SWCNT networks have been recognized as promising forms of nanomaterial for transparent conducting films (TCFs), sensors, and field effect transistors (FETs). To realize high performance complementary metal-oxide semiconductor (CMOS) applications, it is necessary to meet the prerequisites for each transistor cell, that is, high mobility, large on/off ratio, and desired electrical type (n- or p-type property). Several studies have endeavored to improve the performance of FETs by a preferential growth of semiconducting tubes, or a separation of semiconducting SWCNTs using various chemical processes, or by a directional growth or texturing of SWCNT network channels formed by the self-assembly method.[1−4] Doping SWCNTs has been one of the most important issues to be solved in the fundamental studies and application of these materials. SWCNTs exhibit p-type characteristics under ambient conditions due to an oxygen molecule adsorption effect either on the nanotubes or metal electrode.[5−7] A variety of approaches to control the electrical properties of SWCNT FETs have been reported, such as control by depositing organic or inorganic doping layers on the SWCNT surface,[8−12] by changing the work function of metal electrodes,[13,14] or by atomic doping during the synthesis.[15−17] For practical purposes, some requirements for developing doping layers to control the electrical properties of SWCNTs must be taken into account such as (i) controllability in the doping area, (ii) stability under ambient conditions, and (iii) compatibility with Si-based device technologies such as top-gate processes, *etc*. The electronic properties of SWCNTs doped using organic material such as PEI (poly(ethyleneimine)), PAA (poly(acrylic acid)), NADH (*b*-nicotinamide adenine dinucleotide, reduced dipotassium salt), and viologen were found to be degradable over time under ambient conditions.[8−11] Furthermore, organic dopants are not temperature resistant even at temperatures as low as 150 °C, which is fairly low for device applications. Thus, inorganic layers, such as metal or metal oxide seem to be favorable in terms of environmental and thermal stability. Several studies on doping SWCNTs using carbon-free inorganic material have reported that the doping mechanism can be understood by charge transfer due to the difference of electron affinity between the dopant and SWCNTs.[15,18−20] However, doping area selectivity and compatibility

*Address correspondence to jaeyoung88.choi@saumsung.com, jongkim@samsung.com.

Received for review November 10, 2010 and accepted December 27, 2010.

Published online January 24, 2011
10.1021/nn103055u

© 2011 American Chemical Society

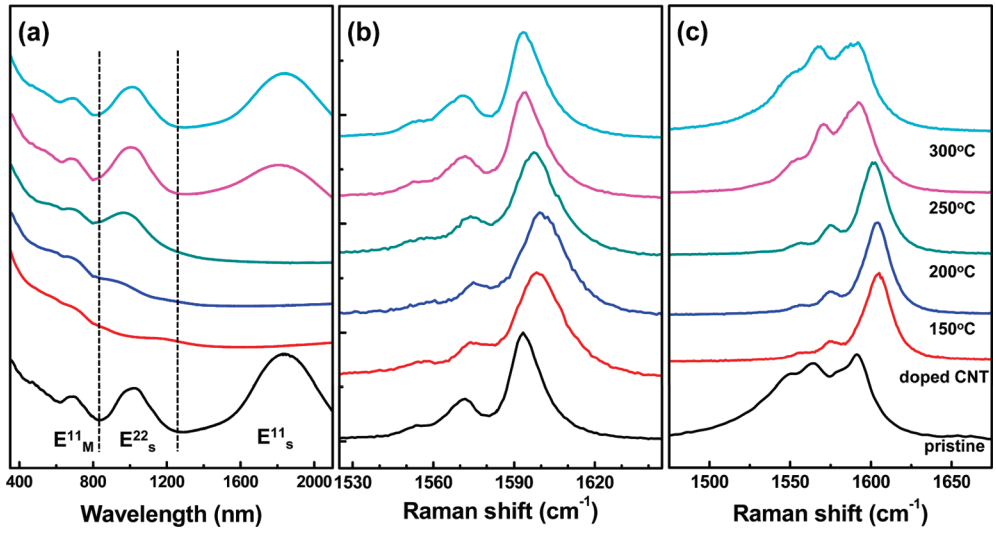

Figure 1. The (a) UV−vis−NIR absorbance spectra and the Raman spectra at an excitation of (b) 514 and (c) 633 nm of as-prepared SWCNTs, $AuCl_3$-doped SWCNTs, and doped SWCNTs after being annealed at various temperatures for 30 min under Ar atmosphere. Spectrum from pristine, 10 mM $AuCl_3$-doped SWCNTs and 10 mM $AuCl_3$-doped SWCNTs followed by annealing at 150, 200, 250, and 300 °C are stacked from bottom to top.

with further device processing involving heating still remained a problematic issue.

In this report, we have demonstrated the environmentally stable and permanent modulation of the electronic and electrical properties of SWCNTs from p-type to ambi-polar and possibly to n-type using an inorganic atomic layer involving heat treatment from 150 to 300 °C. Conversion of these properties in doped SWCNTs using $AuCl_3$ as a strong p-type dopant has been thermally driven by decomposition of $AuCl_3$, which generates the CNT chlorination reaction. Through a systematic study using UV−vis−NIR spectroscopy, Raman scattering, X-ray photoemission spectroscopy (XPS), and electrical measurements, the electronic and electrical properties of $AuCl_3$-doped SWCNTs are found to be modulated as a function of temperature.

RESULTS AND DISCUSSION

Figure 1 exhibits the (a) UV−vis−NIR absorbance and Raman spectra registered at the wavelengths excitation of (b) 514 nm (2.41 eV) and (c) 633 nm (1.96 eV) to investigate the evolution of the electronic structure of the $AuCl_3$-doped SWCNTs as a function of heat treatment temperature. Spectra of pristine, 10 mM $AuCl_3$-doped SWCNTs, and 10 mM $AuCl_3$-doped SWCNTs followed by annealing at 150, 200, 250, and 300 °C are stacked from bottom to top in Figure 1a−c. As shown in Figure 1a, all van Hove singularity-related transition peaks, that is, first and second electronic transition from semiconducting (S) tubes (E^S_{11} and E^S_{22}) and first electronic transition from metallic (M) tubes E^M_{11}, are clearly observed in the pristine SWCNTs. When SWCNTs are doped with 10 mM $AuCl_3$ without heat treatment, all electronics transitions between van Hove singularities completely disappeared resulting from a strong charge-transfer from the SWCNTs to Au^{3+} due to a large reduction potential of Au^{3+}.[18] As the heat treatment temperature increase, the E^S_{22} and E^M_{11} transition peaks of $AuCl_3$-doped SWCNTs are recovered first, and the E^S_{11} related peak is recovered finally above 250 °C. From these observations, it is seen that the doped SWCNTs maintain strong p-type character at 150 °C and the degree of p-type doping decreases gradually above 150 °C.

Similar behavior has been observed also in resonant Raman scattering spectra in Figure 1b,c. With the diameter distribution of the SWCNT material used for this study, at the excitation energy of 2.41 eV (1.96 eV), only semiconducting nanotubes (both semiconducting and metallic tubes) are selectively excited from SWCNT material, respectively, as shown in Figure 1b,c. Metallic and semiconducting SWCNTs have been found to exhibit different Raman lineshapes for the high frequency Raman-active bands near ~1590 cm^{-1}. Early studies on ensembles of SWCNTs indicated that for some laser excitations, the broadened asymmetric G-band line shape was found to be Breit−Wigner−Fano (BWF) resonance process,[21] which was identified with scattering from metallic tubes and involves an interference between electronic and phonon scattering channels. The G-band was deconvoluted into three narrow Lorentzian G-band components in semiconducting (S) SWCNTs for 2.41 eV excitation, and two narrow G-band components in S-tubes and a broad asymmetric G-band component in M-tubes with BWF line shape for 1.96 eV excitation. The strongest G-band component at ~1590 cm^{-1} is named as G^+-band for convenience. The fitting parameters, that is, peak position and width of G^+-band, and intensity of BWF for 2.41 eV and 1.96 eV excitation energies are summarized

TABLE 1. Various Parameters Obtained after Deconvoluting the G-band of the Raman Spectra: Position and Width of G^+ Peak at an Excitation Energy of 2.41 eV and Position and Width of G^+ Peak and Intensity of BWF at an Excitation Energy of 1.96 eV

	Raman at 2.41 eV		Raman at 1.96 eV		
	position of G^+ (cm^{-1})	width of G^+	position of G^+ (cm^{-1})	width of G^+	intensity of BWF
pristine	1594.3	6.94	1592.2	7.44	0.30
$AuCl_3$-doped	1599.3	10.45	1603.9	9.21	0.04
doping and annealing at 150 °C	1600.7	10.45	1603.9	9.21	0.04
doping and annealing at 200 °C	1597.8	10.45	1603.9	9.21	0.04
doping and annealing at 250 °C	1594.7	7.60	1593.1	8.08	0.10
doping and annealing at 300 °C	1594.7	7.43	1592.8	7.44	0.25

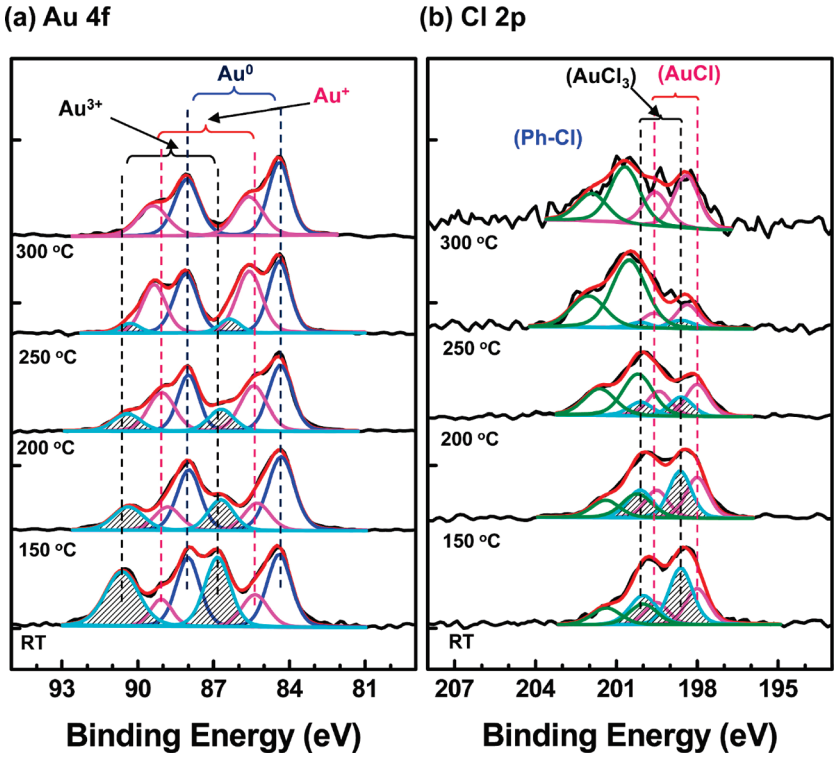

Figure 2. XPS fitted (a) Au 4f and (b) Cl 2p core peaks of the $AuCl_3$-doped SWCNTs annealed at various annealing temperatures.

in Table 1. As shown in Table 1, the G^+-band of $AuCl_3$-doped SWCNTs is up-shifted by ~10 cm^{-1} from 1592 cm^{-1}, and is broadened by ~24% (50%) for 2.41 eV (1.96 eV) laser excitation energy, respectively. This is a typical phenomenon for p-doping effect for SWCNTs.[18,22] The up-shifted position and broadened width of G^+-band induced by $AuCl_3$ doping is maintained up to 200 °C, which agrees well with UV–vis–NIR spectra. Furthermore, the intensity of BWF from M-tubes is observed to be reduced after $AuCl_3$ doping and remains up to 200 °C. With higher annealing temperature above 250 °C, the position and width of G^+-band and the intensity of BWF from M-tubes for doped SWCNTs are almost recovered to that of pristine sample. The observation from the change in Raman spectra evidenced that the p-doping properties of SWCNT networks are stable below 200 °C, and vanish above 250 °C. To confirm this observation, sheet resistance of the doped film has been tested as a function of annealing temperature. Sheet resistance after doping with $AuCl_3$ is reduced by a factor 2. The reduced resistance is maintained stably up to 200 °C and dramatically increased above 250 °C. (see the Supporting Information). The lowered resistance of SWCNT network film by $AuCl_3$ doping originates in an increased carrier density and reduced Schottky barrier height between M- and S-tubes in the SWCNT network.[18] These p-doped statuses were preserved up to 200 °C, which is in agreement with the results from optical studies. This result confirms that the doped SWCNT network film with $AuCl_3$ has good thermal stability in contrast to organic dopants.[23]

To understand the chemical environment change and charge transfer mechanisms in the $AuCl_3$-doped

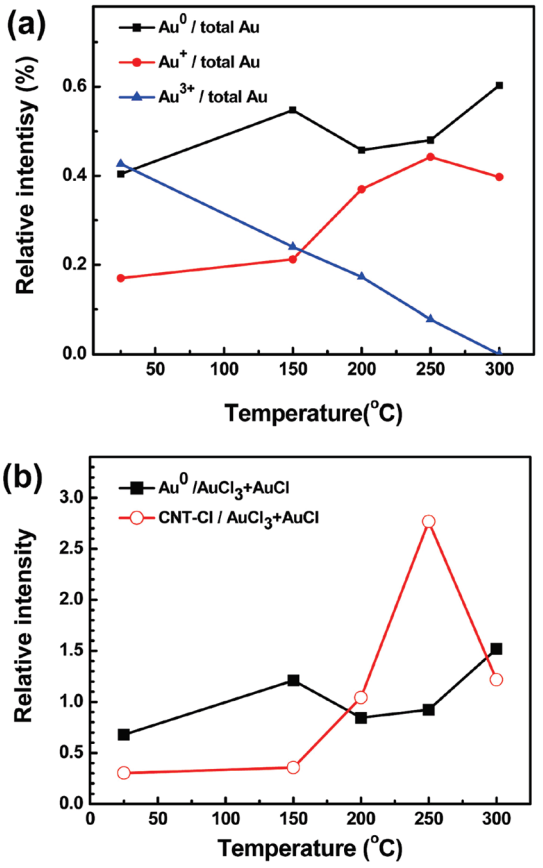

Figure 3. (a) The temperature dependence of relative fraction (Rf) of each Au-containing species at Au 4f and (b) the relative peak intensity of CNT−Cl (Cl 2p) and Au (Au 4f) against gold salts as a function of annealing temperature.

SWCNTs by heat treatment, an XPS study on doped SWCNTs has been undertaken as shown in Figure 2. Both Au 4f and Cl 2p core peaks are probed before and after heat treatment. In the case of doped SWCNTs, the XPS spectrum from Au $4f_{7/2-5/2}$ core level exhibits three doublets associated with $AuCl_3$ (86.7−90.5 eV), AuCl (85.4−89.1 eV), and Au^0 (84.4−88.1 eV), respectively (Figure 2a lower).[24,25] This suggests that Au^{3+} ions are partially reduced to Au^+ and Au^0 due to electron transfer from CNT since the reduction of Au^{3+} is thermodynamically favored due to high redox potential (see the Table 2). This agrees well with the significantly weakened BWF line intensity, upshift of G^+-band in Raman spectrum, and the suppression of the transition band in UV−vis−NIR spectrum (Figure 1).[18,26] In parallel, the XPS Cl $2p_{3/2-1/2}$ core peak is fitted into three doublets attributed to $AuCl_3$ (198.3−199.9 eV), AuCl (198.6−200.0 eV), and phenyl−Cl (199.9−201.3 eV).[24,25] By combining the XPS results from Au 4f and Cl 2p core peaks, the chemical species on the doped SWCNTs are likely to be $AuCl_3$, AuCl, Au^0, and phenyl−Cl (CNT−Cl). At increasing temperature, the peaks associated with $AuCl_3$ at Au 4f and Cl 2p are gradually suppressed.

To track quantitatively the changes in the amount of the adsorbed chemical species on the doped CNTs, that is, $AuCl_3$, AuCl, Au, and CNT−Cl, we systematically registered the evolution of Au 4f and Cl 2p core peaks as a function of annealing temperature. The temperature dependence of relative fraction (Rf) of each Au-related species was measured and plotted as shown in Figure 3a (here, Rf = XPS peaks area of the Au related species/sum of total Au 4f area). The Rf of $AuCl_3$ decreases while the AuCl and Au increase for higher annealing temperature. However at the temperature of 300 °C, the $AuCl_3$ related peaks (Au 4f and Cl 2p) disappeared completely. We assumed that the disappearance of $AuCl_3$ portion in doped SWCNTs annealed at 300 °C is associated with decomposition and/or conversion into AuCl and Au. Between 250 and 300 °C, the suppression of the AuCl portion and the enhancement of the Au^0 relative fraction suggest that the remained AuCl are thermally converted into Au, which agrees with the decomposition of AuCl at about 289 °C.[26] To compare the amount of CNT−Cl and Au concentration, we have plotted the relative peak intensity ratio of CNT−Cl(Cl 2p) and Au^0 (Au 4f) against the summation of peak intensity of $AuCl_3$ and AuCl as a function of annealing temperature as shown in Figure 3b. This may provide an insight on the dominant doping type in $AuCl_3$-doped SWCNTs at each temperature. Regarding the Cl 2p peak, besides the change in the doublets associated with AuCl and $AuCl_3$, the fraction of CNT−Cl increased with higher annealing temperature as consequence of covalent fixation of the byproduct by decomposition of gold chloride at the surface of CNT. Finally, it exhibited an abrupt downturn above 250 °C, and it is presumed that the chlorination reactivity is decreased by a significant loss of $AuCl_3$ and CNT−Cl is decomposed by heat.

TABLE 2. Summary of Reactions at Each Step

step	reaction	products
doping step	$Au^{3+} + 3e^- \rightarrow Au^0$ (s) ($E^0 = 1.498$)[a]	Au
	$Au^{3+} + 2e^- \rightarrow Au^+$ ($E^0 = 1.401$)[a]	AuCl
	$Au^{3+} + 3Cl^- \rightarrow AuCl_3$	$AuCl_3$
	$CNT^+ + Cl^- \rightarrow CNT-Cl$	CNT−Cl
heating step	$AuCl_3 \rightarrow Au + AuCl + Cl_2$ (>160 °C)[26]	Au, AuCl
	$AuCl \rightarrow Au + Cl_2$ (>289 °C)[26]	Au
	$CNT + AuCl_3 + Cl_2 \rightarrow CNT-Cl$[b]	CNT−Cl

[a] Standard redox potential. [b] Chlorination reaction: Aromatic compounds can be chlorinated by treatment with chlorine in the presence of a catalyst, most often iron. However the real catalyst is not the iron itself, but the ferric chloride formed in small amounts from the reaction between iron and the reagent. Ferric chloride and other Lewis acids are often directly used as catalysts.[27]

We have summarized the possible reactions deduced from XPS analysis at each step in Table 2. At the initial doping step, Au^{3+} is partially reduced by charge transfer from CNTs, producing AuCl and Au. Furthermore, residual Cl ions may interact with doped CNTs for charge compensation. During heating steps, the adsorbed $AuCl_3$ is

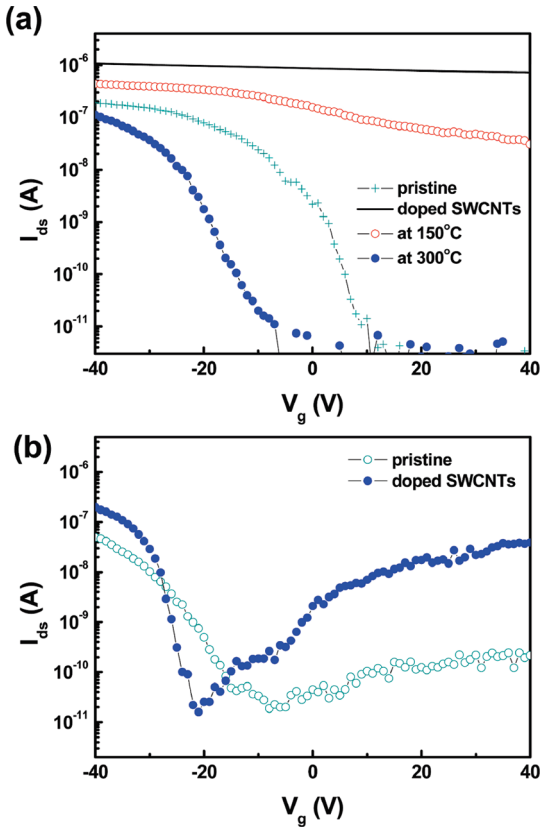

Figure 4. (a) Drain current (I_{ds})−gate voltage (V_g) curve of $AuCl_3$-doped SWCNT network transistor: original (+), 1 mM $AuCl_3$ doped (solid line), annealed at 150 °C (○), and annealed at 300 °C (●) for 30 min and (b) gate voltage dependence on drain current of pristine SWCNTs and $AuCl_3$-doped SWCNTs which are passivated by Al_2O_3 deposited at 300 °C (drain voltage 0.1 V).

thermally decomposed into AuCl, Au, and Cl_2. Of course, a significant amount of Au^{3+} ions involved in CNT doping will be thermally reduced at above 200 °C. Thermally assisted chlorination of CNTs can occur in the presence of $AuCl_3$ and Cl_2, which makes the movement of lone-pair electrons of chlorine back toward the delocalized CNTs because of resonance effect even with high electron negativity of chlorine.[27] This mechanism can explain how the n-type doping characteristics of $AuCl_3$-doped SWCNTs can be thermally induced above 250 °C. At low temperature, strong p-doping effect by charge transfer from Au^{3+} to CNTs is dominant. With higher temperature, the gold species are thermally reduced and thermally induced CNT−Cl bonds are finally formed.

Doping status and the majority carrier type of SWCNTs induced by $AuCl_3$ doping and heat-treatment have been investigated by electrical measurement carried out of SWCNT network transistors. Figure 4a shows the gate voltage dependence (V_g) of drain current (I_{ds}) at each step of doping process, that is, pristine (+), 1 mM $AuCl_3$-doped (solid line), annealed at 150 °C (○), and annealed at 300 °C (●) for 30 min. The annealing was performed under a vacuum with a rotary pump with Ar flow. In Figure 4b, the transfers curve of Al_2O_3 passivated SWCNT transistors with $AuCl_3$ doping (●) and without doping (○) are compared. The 50 nm Al_2O_3 passivation layer, which can be also used as top-gate dielectric, was formed by the atomic layer deposition (ALD) method at 300 °C with trimethyl aluminum (TMA) and water as the precursor and oxidation reagent, respectively. The drain current (I_{ds}) *versus* gate voltage (V_g) curve was measured at the drain voltage (V_{ds}) = 0.1 V (Agilent 4156C). The transistor with pristine SWCNT channel material exhibits p-type behavior under air as reported previously (+ in Figure 4a), due to oxygen adsorption effect on the SWCNT surface. With p-doping by Au^{3+} ions, the on-current level is increased by ~20%. Interestingly, the gating phenomenon has almost disappeared due to the p-doping effect. Moreover, the *I*−*V* transfer curve ends up with that of "artifact conductor" which was found to be due to adsorption of water molecules by $AuCl_3$ salt.[28] The work function change (Fermi level shift) as a function of $AuCl_3$ doping concentration was systematically investigated by using ultraviolet photoelectron spectroscopy (UPS).[18] With 10 mM of doping concentration, the Fermi level can be shifted to a lower value by ~0.15 eV. Above 10 mM, the Fermi level is lowered below the highest valence band. Thus, complete disappearance of the first electronic transition from the semiconducting tubes (E^S_{11}) was observed by UV−vis−NIR spectroscopy.[18] At this point, further studies including Hall measurement need to be done to understand the relationship between the doping level and carrier concentration, which is important for process optimization and device fabrication.

Systematic studies of the doping effect on SWCNT network transistors as a function of $AuCl_3$ concentration, which may induce surface disorders resulting in mobility degradation, are shown in the previous work.[28] With an increase in the doping concentration from 0.1 mM up to ~14 mM of $AuCl_3$, an increase in the disorder induced band (D-band) intensity was observed at concentrations as high as 10 mM. At the concentration of 1 mM, the D-band intensity increase was negligible. The calculated field effect mobilities as a function of doping concentration based on the transfer curve (gate voltage (V_g) dependence on drain current (I_d)) did not exhibit any consistent results. The doping effect on the transport properties of SWCNT network transistors may not be easy to understand due to its complicated components to be considered such as source/drain-carbon nanotube junction, gate oxide and SWCNT interface, and tube−tube junctions, *etc.* However, at the highest doping concentration (~14 mM) mobility has been dramatically increased even though D-band intensity is shown to be enhanced. With large doping concentration, the mobility enhancement effect due to increased carrier density seems to be dominant over degradation by surface disorder creation. From Raman studies and mobility change, surface disorder

induced by chemical doping seems to have a weak relation to device mobility, or mobility degradation due to surface disorder creation might be less dominant over mobility enhancement by increased carrier density.

The on/off ratio of the $AuCl_3$-doped SWCNT network transistor is partially (or fully) recovered when annealed at 150 °C (○) (300 °C (●)) for 30 min under vacuum with Ar flow. The *I*−*V* measurements were done under air. These results agree well with UV−vis−NIR, Raman, and XPS results shown in the previous section, that the p-doping status of $AuCl_3$-doped CNTs disappeared by heat treatment above 250 °C. The thermally induced majority carrier-type conversion of $AuCl_3$-doped SWCNT transistor was confirmed by comparing the passivation effect on the *I*−*V* characteristics of undoped and $AuCl_3$-doped SWCNT transistors as shown in Figure 4b. The results for Figure 4a,b are from different sets of SWCNT devices. Thus, the doping level by the same $AuCl_3$ concentration can appear to be different. The $AuCl_3$-doped SWCNT transistor with 50 nm Al_2O_3 passivation layer clearly exhibits ambi-polar characteristics in contrast with the undoped SWCNT transistor case which is closer to the p-type. This observation agrees well with XPS results shown in the previous section. The P-doping effect disappeared due to thermal reduction of the gold species. Instead, an n-type doping effect from thermally assisted chlorination of CNTs becomes important. Under ambient atmosphere, due to an oxygen adsorption effect on the carbon nanotube surface, electrons are trapped resulting in p-type characteristics.[6,7,29] By Al_2O_3 passivation on the $AuCl_3$-doped SWCNT network after annealing at 300 °C, adsorbed oxygen molecules will be desorbed from the SWCNT body and prevented from re-adsorption, which will induce clear ambi-polar characteristics with high n-current for $AuCl_3$-doped SWNTs with *in situ* heat treatment. It is an interesting result from the application point of view that the polarity of SWCNT transistors can be modulated by a $AuCl_3$ doping conditions on SWCNTs, that is, $AuCl_3$ doping concentration and heat treatment. More importantly, since the doping scheme is based on carbon-free inorganic material, it has the benefits of environmental stability and compatibility with further device processing involving heat treatment. To confirm that the n-type doping effect is dominated from thermally assisted chlorination of CNTs, not from charge transfer from Al_2O_3 layer, we have performed several experiments.

In one experiment, we compared the Hall coefficient (RHs) for an undoped and doped SWCNT network thin film before and after 250 °C annealing. We clearly observed that RHs is converted from a positive to a negative value for a 10 mM $AuCl_3$-doped SWCNT network after 250 °C annealing (from $+0.000613$ m^2/C to -0.00216 m^2/C). In the case of undoped SWCNT network, the RHs remains constant before and after annealing at 250 °C ($+0.000613$ m^2/C). Even though RHs values for the doped and undoped SWCNT network are measured to be the same, the carrier concentration for the doped SWCNT network is found to be several times higher than for the undoped SWCNT network. This is consistent with Raman, UV−vis−NIR, XPS, and *I*−*V* results. Finally, a negative Hall coefficient is maintained at least for 6 months with slight degradation (-0.00133 m^2/C), possibly due to the p-doping effect from oxygen adsorption under ambient conditions.[5−7] Different from organic doping, chlorination of SWCNTs by our approach is much more stable under ambient conditions.

CONCLUSIONS

By comprehensive studies using UV−vis−NIR, Raman, XPS, and *I*−*V* measurements, we evidenced the electronic and electrical conversion of $AuCl_3$-doped SWCNT network by thermal annealing. At low annealing temperatures, a strong p-doping effect from the Au^{3+} ions to the CNTs due to a large difference in reduction potential between them is dominant. However at higher temperature, the gold species are thermally reduced, and thermally induced CNT−Cl finally occurs. Thus, in the $AuCl_3$-doped SWCNTs treated at higher annealing temperature, the p-type doping effect is suppressed and the n-type property from CNT−Cl is thermally induced. We have demonstrated a doping scheme that is environmentally stable and compatible with further device processing and that involves carbon-free inorganic material to modulate the majority carrier type conversion from p-type to ambi-polar, and possibly to n-type, by $AuCl_3$ doping conditions on SWCNTs.

EXPERIMENTAL SECTION

Method of preparing and doping SWCNT network thin films: Arc discharge SWCNTs purchased from Iljin Nanotech Co., Ltd. were used in this study. SWCNTs were dispersed in 0.1 wt % NaDDBS aqueous solution using a bath sonicator (Bandelin Sonorex, 240 W for 10 h) and centrifuged to get a well-dispersed solution. The SWCNT network thin films on silicon wafer were sprayed using a solution (ncs-200, NCS co,. Ltd., Korea) and then washed in 15% HNO_3 solution. A $AuCl_3$ solution of 10 mM was dissolved in nitromethane and dropped onto the prepared SWCNT films. After 30 s of residual time, the solvent was spin-coated at 2500 rpm for 30 s to remove residual $AuCl_3$ and solvent. (Midas System, Spin 2000). The doped SWCNT films were annealed at 150, 200, 250, and 300 °C for 30 min under Ar atmosphere with a rotary pump.

SWCNT network transistor fabrication procedure:[30] SWCNT networks were grown by water−methane (CH_4) plasma assisted chemical vapor deposition at 450 °C on SiO_2 (4000 Å)/Si substrates using a direct photolithographic technique that employed a simple mixture of ferrocene and commercially

available photoresist. We have used 0.01 M of ferrocene in the resist to obtain the density of 25 tubes per μm^2 with ~0.5 μm of the nanotube length. Another photolithography process was followed to form source (S) and drain (D) electrodes on the arrayed SWNT network channels. Ti (100 nm) was used as the electrode material. The SWCNT network was doped with 1 mM $AuCl_3$ solution and annealed at 150 and 300 °C for 30 min under Ar atmosphere with rotary pump. Successive introduction of trimethyl aluminum (TMA) as precursor and water as oxidation reagent was repeated to form the 50 nm Al_2O_3 layer by atomic layer deposition (ALD) method at 300 °C with rotary pump condition and Ar flow for purge.

Measurement: The doped SWCNT films before and after heat-treatment were characterized by XPS analysis by using a monochromatized Al Kα radiation (1486.6 eV) (QUANTUM 2000, Physical electronics), and micro-Raman spectroscopy (Renishaw InVia Reflex). Measurements of the sheet resistance were carried out by four-point probe method (Keithley 2000). $I-V_g$ characteristics were measured with a parameter analyzer (Agilent 4156C) using a probe station under ambient conditions. The sheet carrier density, mobility, Hall coefficient, and sheet resistance of graphene were measured by the van der Pauw method using a Hall measurement (ACCENT semiconductor UK/HL 5500PC) at room temperature, 0.3 T.

Supporting Information Available: The sheet resistance of a doped SWCNT transparent conducting film as function of temperature. This material is available free of charge *via* the Internet at http://pubs.acs.org.

REFERENCES AND NOTES

1. Hong, G.; Zhang, B.; Peng, B.; Zhang, J.; Choi, W. M.; Choi, J.-Y.; Kim, J. M.; Liu, Z. Direct Growth of Semiconducting Single-Walled Carbon Nanotube Array. *J. Am. Chem. Soc.* **2009,** *131*, 14642–14643.
2. LeMieux, M. C.; Roberts, M.; Barman, S.; Jin, Y. W.; Kim, J. M.; Bao, Z. Self-Sorted, Aligned Nanotube Networks for Thin-Film Transistors. *Science* **2008,** *321*, 101–104.
3. Kocabas, C.; Hur, S.-H.; Gaur, A.; Meitl, M. A.; Shim, M.; Rogers, J. A. Guided Growth of Large-Scale, Horizontally Aligned Arrays of Single-Walled Carbon Nanotubes and Their Use in Thin-Film Transistors. *Small* **2005,** *1*, 1110–1106.
4. Lee, M.; Noah, M.; Park, J.; Seong, M.-J.; Kwon, Y.-K.; Hong, S. Textured" Network Devices: Overcoming Fundamental Limitations of Nanotube/Nanowire Network-Based Devices. *Small* **2009,** *5*, 1642–1648.
5. Heinze, S.; Tersoff, J.; Martel, R.; Derycke, V.; Appenzeller, J.; Avouris, P. Carbon Nanotubes as Schottky Barrier Transistors. *Phys. Rev. Lett.* **2002,** *89*, 106801.
6. Derycke, V.; Martel, R.; Appenzeller, J.; Avouris, P. Controlling Doping and Carrier Injection in Carbon Nanotube Transistors. *App. Phys. Lett.* **2002,** *80*, 2773–2775.
7. Kang, D.; Park, N.; Hyun, J.; Bae, E.; Ko, J.; Kim, J.; Park, W. Adsorption-Induced Conversion of the Carbon Nanotube Field Effect Transistor from Ambipolar to Unipolar Behaviour. *App. Phys. Lett.* **2005,** *86*, 093105.
8. Shim, M.; Javey, A.; Kam, N. W. S.; Dai, H. Polymer Functionalization for Air-Stable n-Type Carbon Nanotube Field-Effect Transistors. *J. Am. Chem. Soc.* **2001,** *123*, 11512–11513.
9. Siddons, G. P.; Merchin, D.; Back, J. H.; Jeong, J. K.; Shim, M. Highly Efficient Gating and Doping of Carbon Nanotubes with Polymer Electrolytes. *Nano Lett.* **2004,** *4*, 927–931.
10. Kang, B. R.; Yu, W. J.; Kim, K. K.; Park, Y. J.; Kim, G.; Shin, H.-J.; Kim, U. J.; Lee, E.-H.; Choi, J.-Y.; Lee, Y. H. Restorable Type Conversion of Carbon Nanotube Transistor using Pyrolytically Controlled Antioxidizing Photosynthesis Coenzyme. *Adv. Funct. Mater.* **2009,** *19*, 2553–2559.
11. Kim, S. M.; Jang, J. H.; Kim, K. K.; Park, H. K.; Bae, J. J.; Yu, W. J.; Lee, I. H.; Kim, G.; Loc, D. D.; Kim, U. J.; *et al.* Reduction-Controlled Viologen in Bisolvent as an Environmentally Stable n-Type Dopant for Carbon Nanotubes. *J. Am. Chem. Soc.* **2009,** *131*, 327–331.
12. Wang, Z.; Xu, H.; Zhang, Z.; Wang, S.; Ding, L.; Zeng, Q.; Yang, L.; Pei, T.; Liang, X.; Gao, M.; *et al.* Growth and Performance of Yttrium Oxide as an Ideal High-κ Gate Dielectric for Carbon Based Electronics. *Nano Lett.* **2010,** *10*, 2024–2030.
13. Kim, H.-S.; Kim, B.-K.; Kim, J.-J.; Lee, H.-O.; Park, N. J. Controllable Modification of Transport Properties of Single-Walled Carbon Nanotube Field Effect Transistors with *in Situ* Al Decoration. *Appl. Phys. Lett.* **2007,** *91*, 153113.
14. Zhang, Z.; Liang, X.; Wang, S.; Yao, K.; Hu, Y.; Zhu, Y.; Chen, Q.; Zhou, W.; Li, Y.; Yao, Y.; *et al.* Doping-free Fabrication of Carbon Nanotube Based Ballistic CMOS Devices and Circuits. *Nano Lett.* **2007,** *7*, 3603–3607.
15. Liu, X. M.; Romero, H. E.; Gutierrez, H. R.; Adu, K.; Eklund, P. C. Transparent Boron-Doped Carbon Nanotube Films. *Nano Lett.* **2008,** *8*, 2613–2619.
16. Min, Y.-S.; Bae, E.; Asanov, I. P.; Kim, U. J.; Park, W. Growth and Characterization of Nitrogen-Doped Single-Walled Carbon Nanotube by Water-Plasma Chemical Vapour Deposition. *Nanotechnology* **2007,** *28*, 285601.
17. Maciel, I. O.; Campos-Delgado, J.; Cruz-Silva, E.; Pimenta, M. A.; Sumpter, B. G.; Meunier, V.; Lpez-Uras, F.; Muoz-Sandoval, E.; Terrones, H.; Terrones, M.; *et al.* Synthesis, Electronic Structure, and Raman Scattering of Phosphorus-Doped Single-Wall Carbon Nanotubes. *Nano Lett.* **2009,** *9*, 2267–2272.
18. Kim, K. K.; Bae, J. J.; Park, H. K.; Kim, S. M.; Geng, H.; Park, K. A.; Shin, H.-J.; Yoon, S.-M.; Benayad, A.; Choi, J.-Y.; *et al.* Fermi Level Engineering of Single-Walled Carbon Nanotubes by $AuCl_3$ Doping. *J. Am. Chem. Soc.* **2008,** *130*, 12757–12761.
19. Yoon, S.-M.; Kim, S. J.; Shin, H.-J.; Benayad, A.; Choi, S. J.; Kim, K. K.; Kim, S. M.; Park, Y. J.; Kim, G.; Choi, J.-Y.; *et al.* Selective Oxidation on Metallic Carbon Nanotubes by Halogen Oxoanions. *J. Am. Chem. Soc.* **2008,** *130*, 2610–2616.
20. Shin, H.-J.; Kim, S. M.; Yoon, S.-M.; Benayad, A.; Kim, K. K.; Kim, S. J.; Park, H. K.; Choi, J.-Y.; Lee, Y. H. Tailoring Electronic Structures of Carbon Nanotubes by Solvent with Electron-Donating and -Withdrawing Groups. *J. Am. Chem. Soc.* **2008,** *130*, 2062–2066.
21. Kim, U. J.; Gutiérrez, H. R.; Gupta, A. K.; Eklund, P. C. Raman Scattering Study of the Thermal Conversion of Bundled Carbon Nanotubes into Graphitic Nanoribbons. *Carbon* **2008,** *46*, 729–740.
22. Rao, A. M.; Eklund, P. C.; Bandow, S.; Thess, A.; Smalley, R. E. Evidence for Charge Transfer in Doped Carbon Nanotube Bundles from Raman Scattering. *Nature* **1997,** *388*, 257–259.
23. Jackson, R.; Domercq, B.; Jain, R.; Kippelen, B.; Graham, S. Stability of Doped Transparent Carbon Nanotube Electrodes. *Adv. Funct. Mater.* **2008,** *18*, 2548–2554.
24. Wagner, C. D.; Riggs, W. M.; Davis, L. E.; Moulder, J. F.; Muilenberg, G. E. In *Handbook of X-ray Photoelectron Spectroscop*; Perkin−Elmer Corporation: Covina, CA, 1978.
25. Benayad, A.; Shin, H.-J.; Park, K.; Yoon, S.-M.; Kim, K. K; Jin, M. H.; Jeong, H.-K.; Lee, J. C.; Choi, J.-Y.; Lee, Y. H. Controlling Work Function of Reduced Graphite Oxide with Au-Ion Concentration. *Chem. Phys. Lett.* **2009,** *475*, 91–95.
26. In *The Merck Index: An Encyclopedia of Chemicals, Drugs and Biologicals*; Budavari, S., O'Neil, M. J., Smith, A., Heckelman, P. E., Kinnenry, J. F., Eds.; Merck & Co.: Whitehouse Station, NJ, 1996; Vol. 2.
27. March, J. In *Advanced Organic Chemistry:Reactions, Mechanisms, and Structure*; Wiley-Interscience: New York, 1992; Chapter 2, 9.
28. Lee, I. H.; Kim, U. J.; Son, H. B.; Yoon, S.-M.; Yao, F.; Yu, W. J.; Duong, D. L.; Choi, J.-Y.; Kim, J. M.; Lee, E. H.; *et al.* Hygroscopic Effects on $AuCl_3$-Doped Carbon Nanotubes. *J. Phys. Chem. C* **2010,** *114*, 11618–11622.
29. Heinze, S.; Tersoff, J.; Martel, R.; Derycke, V.; Appenzeller, J.; Avouris, P. Carbon Nanotubes as Schottky Barrier Transistors. *Phys. Rev. Lett.* **2002,** *89*, 106801.
30. Kim, U. J.; Lee, E. H.; Kim, J. M.; Min, Y.-S.; Kim, E.; Park, W. Thin Film Transistors Using Preferentially Grown Semiconducting Single-Walled Carbon Nanotube Networks by Water-Assisted Plasma-Enhanced Chemical Vapour Deposition. *Nanotechnology* **2009,** *20*, 295201.